

Draft: April 29, 2003

# Accretion Disk Spectra of the Ultra-luminous X-ray Sources in Nearby Spiral Galaxies and Galactic Superluminal Jet Sources

Ken Ebisawa<sup>1</sup>

*code 662, NASA/GSFC, Greenbelt, MD 20771, USA*

*and*

*INTEGRAL Science Data Centre, chemin d'Écogia 16, Versoix, 1290 Switzerland*

`ebisawa@obs.unige.ch`

Piotr Życki

*N. Copernicus Astronomical Center, Bartycka 18, 00-716 Warsaw, Poland*

Aya Kubota

*Institute of Space and Astronautical Science, 3-1-1 Yoshinodai, Sagamihara, Kanagawa,  
229-8510 Japan*

Tsunefumi Mizuno

*Department of Physics, Hiroshima University, 1-3-1, Kagamiyama, Higashi-Hiroshima,  
Hiroshima, 739-8526 Japan*

*and*

Ken-ya Watarai

*Department of Astronomy, Graduate School of Science, Kyoto University, Sakyo-ku, Kyoto,  
606-8502 Japan*

## ABSTRACT

Ultra-luminous Compact X-ray Sources (ULXs) in nearby spiral galaxies and Galactic superluminal jet sources share the common spectral characteristic that they have unusually high disk temperatures which cannot be explained in the

---

<sup>1</sup>Universities Space Research Association.

framework of the standard optically thick accretion disk in the Schwarzschild metric. On the other hand, the standard accretion disk around the Kerr black hole might explain the observed high disk temperature, as the inner radius of the Kerr disk gets smaller and the disk temperature can be consequently higher. However, we point out that the observable Kerr disk spectra becomes significantly harder than Schwarzschild disk spectra *only when* the disk is highly inclined. This is because the emission from the innermost part of the accretion disk is Doppler-boosted for an edge-on Kerr disk, while hardly seen for a face-on disk. The Galactic superluminal jet sources are known to be highly inclined systems, thus their energy spectra may be explained with the standard Kerr disk with known black hole masses. For ULXs, on the other hand, the standard Kerr disk model seems implausible, since it is highly unlikely that their accretion disks are preferentially inclined, and, if edge-on Kerr disk model is applied, the black hole mass becomes unreasonably large ( $\gtrsim 300M_{\odot}$ ). Instead, the slim disk (advection dominated optically thick disk) model is likely to explain the observed super-Eddington luminosities, hard energy spectra, and spectral variations of ULXs. We suggest that ULXs are accreting black holes with a few tens of solar mass, which is not unexpected from the standard stellar evolution scenario, and their X-ray emission is from the slim disk shining at super-Eddington luminosities.

*Subject headings:* superluminal jet sources: ultra-luminous X-ray sources: accretion disks, slim disks: Schwarzschild black holes, Kerr black holes

## 1. Introduction

Ultra-luminous compact X-ray sources (ULXs) have been found in nearby spiral Galaxies, with typical 0.5 – 10 keV luminosities  $10^{39}$  to  $10^{40}$  erg s $^{-1}$  (e.g., Fabbiano 1988; Colbert and Mushotzky 1999; Makishima et al. 2000; Colbert and Ptak 2002; Foschini et al. 2002). These luminosities are too small for AGNs, and most ULXs are in fact located significantly far from the photometric center of the galaxies. On the other hand, ULXs are too luminous to be considered as the same class of the compact binary X-ray sources in our Galaxy whose luminosities are almost always  $\lesssim 10^{39}$  erg s $^{-1}$ .

Significant time variations have been detected from ULXs, and their energy spectra are successfully modeled with emission from optically thick accretion disks (Okada et al. 1998; Mizuno et al. 1999; Kotoku et al. 2000; Makishima et al. 2000; Mizuno, Kubota and Makishima 2001), as is the case for the “High” state (= Soft-state) of Galactic black hole candidates (e.g., Tanaka and Lewin 1995). In addition, discovery of bimodal spectral

transitions (Kubota et al. 2001) and orbital modulations (Bauer et al. 2001; Sugiho et al. 2001) from several ULXs further demonstrate their resemblance with Galactic black hole candidates. These observational facts suggest that ULXs are moderately massive black holes, which may be scale-up versions of the Galactic black holes. So that the observed luminosities of ULXs,  $\sim 10^{40}$  erg s $^{-1}$ , do not exceed the Eddington limit  $L_{Edd} = 1.5 \times 10^{38} (M/M_{\odot})$  erg s $^{-1}$ , the black hole mass has to be as large as or greater than  $\sim 100 M_{\odot}$ , assuming isotropic emission. How to create such “intermediate” mass black holes, if truly exist, is an intriguing question (e.g., Ebisuzaki et al. 2001). On the other hand, if X-ray emission is unisotropic, the black hole mass is not required to be so large. For example, a beaming model for ULXs has been proposed (King et al. 2001; Körding, Falcke and Markoff 2002); however, presence of a bright nebula surrounding M81 X-9 (Wang 2002) suggests that the nebula is powered by the central X-ray source and that strong X-ray beaming is rather unlikely. Another possibility to solve the super-Eddington problem through unisotropic emission is a geometrically thick accretion disk (Watarai, Mizuno and Mineshige 2001), which we favorably consider later (section 4.1).

GRS 1915+105 and GRO J1655–40 are the two well-known Galactic superluminal jet sources and established black hole binaries with reliable mass measurements ( $M \approx 7M_{\odot}$  for GRO J1655–40 [Orosz and Bailyn 1997] and  $\approx 14M_{\odot}$  for GRS 1915+40 [Greiner, Cuby and McCaughrean 2001]). If soft X-ray energy spectra of these sources are fitted with an optically thick accretion disk model, their characteristic disk temperatures are  $\sim 1.3 - 2.0$  keV (e.g., Belloni et al. 1997; Zhang et al. 1997; Zhang, Cui and Chen 1997; Tomsick et al. 1999). These values are systematically higher than those of ordinary and well-studied soft-state black hole candidates such as Cyg X-1 and LMC X-3, whose disk temperatures are almost always less than  $\sim 1$  keV (e.g., Tanaka and Lewin 1995).

Okada et al. (1998) found that a luminous ULX in IC342 ( $\sim 2 \times 10^{40}$  erg s $^{-1}$ ; “Source 1”) has unusually high disk temperature ( $\sim 1.7$  keV), which is similar to the accretion disk spectra of Galactic superluminal jet sources, and pointed out that such a high disk temperature cannot be explained in the framework of the “standard” accretion disk around a Schwarzschild black hole (see section 2.1 and 3.2). The “standard” disk denotes the situation that all the gravitational energy release is converted to thermal radiation, in contrast to the “slim” disk which is an optically and geometrically thick disk with dominant energy advection (section 4.1). Makishima et al. (2000) summarized ASCA observations of seven ULXs, and concluded that the unusually high accretion disk temperature is a common spectral property of ULXs. Zhang, Cui and Chen (1997) and Makishima et al. (2000) suggested that the unusually high disk temperature of the Galactic superluminal jet sources and ULXs may be explained if they harbor fast rotating black holes, since inner edge of the accretion disk gets closer to the black hole in the Kerr geometry and the disk can be hotter. On the

other hand, Watarai et al. (2000) and Watarai, Mizuno and Mineshige (2001) proposed that, instead of the standard disk, the slim disk model may explain the X-ray energy spectra of Galactic superluminal jet sources and ULXs.

In this paper, we focus on the “too-hot disk” problem of ULXs and Galactic superluminal jet sources. We apply standard accretion disk models in Newtonian, Schwarzschild, and Kerr cases, and discuss how the relativistic effects and the disk inclination affect the black hole mass and the mass accretion rates obtained from the model fitting. We see that observed hard spectra of Galactic superluminal jet sources may be explained by strong relativistic effects in the highly inclined Kerr accretion disk. On the other hand, the hard spectra and the super-Eddington problem of ULXs are difficult to explain in the framework of the standard accretion disk model. We see that the slim disk model may explain the observed super-Eddington luminosities and hard energy spectra of ULXs more naturally.

## 2. Characteristics of the Standard Accretion Disk Model

Before quantitative discussion of the observed energy spectra and accretion disk parameters, we summarize important observational characteristics of the standard accretion disk model.

### 2.1. Disk Temperature

Let’s assume a standard optically thick accretion disk (Shakura and Sunyaev 1973) in the Schwarzschild metric, in which case the last stable orbit around the non-rotating black hole is  $6 r_g$ , where the gravitational radius  $r_g \equiv GM/c^2$  is defined. We identify the last stable orbit with the innermost disk radius,  $r_{in}$ . The radial dependence of the “effective” temperature of an optically accretion disk may be written as,

$$T_{eff}(r) = \left\{ \frac{3GM\dot{M}}{8\pi\sigma r^3} R_R(r/r_{in}) \right\}^{1/4}, \quad (1)$$

where  $R_R$  is  $(1 - \sqrt{r_{in}/r})$  in the Newtonian case, otherwise includes additional general relativistic correction (see e.g., Krolik 1999). The effective temperature is zero at  $r = r_{in}$ , peaks at  $r \approx 8 r_g$ , and decreases with  $\propto r^{-3/4}$  outward.

Because of the Comptonization, the color temperature of the local emission becomes higher than the effective temperature, and their ratio is almost constant at  $\approx 1.7$  (section

2.3). Therefore, the observable disk color temperature also peaks at  $r \approx 8r_g$ , and takes the maximum values,

$$T_{col}^{(max)} \approx (1.0 - 1.3) \text{ keV} \left( \frac{T_{col}/T_{eff}}{1.7} \right) \left( \frac{\dot{M}}{\dot{M}_C} \right)^{1/4} \left( \frac{M}{7M_\odot} \right)^{-1/4}, \quad (2)$$

where we define the critical mass accretion rate  $\dot{M}_C \equiv 2.9 \times 10^{18} (M/M_\odot) \text{ g s}^{-1}$ , so that  $\dot{M} = \dot{M}_C$  gives the Eddington luminosity (see appendix A). The small temperature variation reflects the inclination effects (from face-on to  $i = 80^\circ$ ), such that inclined Schwarzschild disks have slightly harder spectra (section 2.4 and Appendix B).

From equation (2), we can see that an optically thick accretion disk around a  $7 M_\odot$  or  $100 M_\odot$  Schwarzschild black hole may not have a higher color temperature than  $\sim 1.3 \text{ keV}$  or  $\sim 0.7 \text{ keV}$ , respectively, unless super-Eddington mass accretion is allowed. To explain higher disk temperatures, either super-Eddington mass accretion rates or unreasonably small mass is required. This is the “too-hot disk” problem of the Galactic superluminal jet sources and ULXs we are concerned in this paper.

## 2.2. Multi-color disk approximation

We point out that the maximum disk color temperature as expressed with (2) is a quantity directly constrained from observations. If we approximate optically thick accretion disk spectra with a simple multicolor disk blackbody model (MCD model; Mitsuda et al. 1994; Makishima et al. 1996) in which local emission is a blackbody and radial dependence of the temperature is simplified as  $T(r) = T_{in} (R_{in}/r)^{3/4}$ , the apparent inner disk radius  $R_{in}$  and temperature  $T_{in}$  will be the independent model parameters<sup>2</sup>, such that the spectral shape is determined only by  $T_{in}$ , and the flux is proportional to  $R_{in}^2 T_{in}^4$ . When observed spectra are fitted with the MCD model,  $T_{in}$  may be identified with the maximum disk color temperature (2), while the true inner disk radius  $r_{in}$  and apparent radius  $R_{in}$  have a relation  $r_{in} \approx 0.4 (T_{col}/T_{eff})^2 R_{in}$  (Kubota et al. 1998).

---

<sup>2</sup>In this paper,  $r_{in}$  denotes the real disk inner radius, while  $R_{in}$  is the apparent inner radius as a MCD model parameter. Appendix C gives conversion formulae between the MCD parameters ( $R_{in}$  and  $T_{in}$ ) and realistic disk parameters ( $M$  and  $\dot{M}$ ) in the Schwarzschild case.

### 2.3. Local Energy Spectra

In the inner part of the optically thick accretion disk, the electron scattering opacity is dominant, and the hot disk atmosphere distorts the emergent spectra via Comptonization. Such precise theoretical calculation of the accretion disk spectra for Galactic black hole candidates has been made by several authors (e.g., Shimura and Takahara 1995; Ross and Fabian 1996; Blaes et al. 2001). These authors basically agree that the local spectrum from each ring of the disk can be approximated by the “diluted black body”,  $(T_{eff}/T_{col})^4 B(E, T_{col})$ , where  $B(E, T_{col})$  is the Planck function with color temperature  $T_{col}$  ( $> T_{eff}$ ), in the  $\sim 0.5 - 10$  keV band (where most observations are relevant). Also, ratio of the color temperature to the effective temperature,  $T_{col}/T_{eff}$ , is virtually constant at  $1.7 - 1.9$  along the disk radius. Hence, equation (2) is valid, and simple MCD approximation is useful to describe observed disk spectra. Throughout this paper, we use  $T_{col}/T_{eff} = 1.7$  to fit the observed spectra.

It should be noted that the mass obtained by fitting the standard accretion disk model to the observed spectra is proportional to  $(T_{col}/T_{eff})^2$ , as long as the diluted black body approximation is valid. This can be readily seen as follows: The accretion disk spectrum may be expressed as,

$$\begin{aligned} & \int_{r_{in}}^{r_{out}} 2\pi r \left( \frac{T_{eff}}{T_{col}} \right)^4 B(E, T_{col}(r, M, \dot{M})) dr \\ & \approx r_{in}^2 \int_{(r/r_{in})=1}^{\infty} 2\pi (r/r_{in}) \left( \frac{T_{eff}}{T_{col}} \right)^4 B(E, T_{col}(r/r_{in}, M, \dot{M})) d(r/r_{in}) \\ & = \left( \frac{6G(T_{eff}/T_{col})^2 M}{c^2} \right)^2 \int_{(r/r_{in})=1}^{\infty} 2\pi (r/r_{in}) B(E, T_{eff}(r/r_{in}, (T_{eff}/T_{col})^2 M, \dot{M})) d(r/r_{in}), \end{aligned} \quad (3)$$

where we have used  $r_{in} = 6GM/c^2$  and  $T_{col} \propto \dot{M}^{1/4} (r/r_{in})^{-3/4} ((T_{eff}/T_{col})^2 M)^{-1/2}$  from equation (1). Equation (3) indicates that the accretion disk spectrum with the black hole mass  $M$  and the diluted black body local spectrum is identical to the disk spectrum with the black hole mass  $(T_{eff}/T_{col})^2 M$  and the black body local spectrum.

### 2.4. Relativistic Effects

Due to the relativistic effects in the Schwarzschild metric, observed disk spectral shape is mildly inclination-angle dependent, such that inclined disk spectra become slightly harder (appendix C, figure 1). This is due to the gravitational redshift and Doppler boosts near the inner edge of the accretion disk. Note that the relativistic effect is not significant outside

of  $6 r_g$ , so that the Schwarzschild disk spectra are not very much different from those of Newtonian disks. This is in contrast to the extreme Kerr case, in which the relativistic effect is enormous near  $r_{in} \approx r_g$  and the disk spectrum is extremely inclination dependent (see below; figure 1 and 2).

While in the Schwarzschild metric the last stable orbit around the black hole is  $6 r_g$ , in the Kerr metric it can go down to  $1.24 r_g$  with an extreme angular momentum of  $a = 0.998$ . As the inner edge of the accretion disk approaches the black hole, more gravitational energy is released, and the inner disk temperature can get higher. X-ray energy spectra from optically thick Kerr accretion disks have been calculated by many authors including Cunningham (1975), Connors, Piran and Stark (1980), Asaoka (1989), Sun and Malkan (1989), Laor, Netzer and Piran (1990), Hubeny et al. (2000) and Gielinski, Maciolek-Niedzwieck and Ebisawa (2001). In this paper, we calculate the Kerr disk spectral model using the transfer function by Laor, Netzer and Piran (1990) for  $a = 0.998$ . To make a comparison easier, we assume  $r_{in} = 1.24 r_g$ , and the same local spectrum as we did for the Schwarzschild disk model (section 2.3), namely diluted black body with  $T_{col}/T_{eff} = 1.7$ .

In Figure 1, we show comparison of the Schwarzschild and Kerr disk spectra, as well as Newtonian one, for the face-on and a highly inclined case ( $i = 80^\circ$ ). The biggest difference between the Kerr disk model and the other two models is the presence or absence of the innermost region of the disk from  $1.24 r_g$  to  $6 r_g$ . When the disk is close to face-on, the contribution from this part is not significant because of the gravitational red-shift and light-bending; as a result, the total Kerr disk spectrum is not very much different from the Newtonian or Schwarzschild ones. On the other hand, emission from the innermost part becomes very significant for a highly inclined disk due to Doppler boosting. Consequently, a near edge-on Kerr disk spectrum comprises a significant amount of high energy X-ray photons compared to the Newtonian or Schwarzschild disks.

Inclination angle dependence of the observed Kerr disk spectrum is different in different energy bands (figure 2). At lower energies, where most of the emission is from the outer parts of the disk ( $r > 400 r_g$ ), the flux is proportional to the projected disk area and decreases with inclination, just as Newtonian disks. On the other hand, higher energy fluxes from the innermost parts of the disk ( $1.26 r_g < r < 7 r_g$ ) are *enhanced* as the disk is more inclined, due to strong Doppler boosting. Consequently, inclined Kerr disks are *brighter* than the face-on disks in the highest energy bands, as previous authors have already pointed out.

### 3. Application of the Standard Disk Model

We apply the standard accretion disk spectral models to ASCA archival data of GRO J1655–40 and IC342 Source 1. The observations were made on 1995 August for GRO J1655–40 (when the source is in a bright state) and 1993 September for IC342 Source 1. These datasets may be considered “exemplary”, so that the same spectral data of GRO J1655–40 have been analyzed in Zhang et al. (1997), Zhang et al. (2000) and Gieliński, M., Maciolek-Niedzwiecki, A. and Ebisawa, K. (2001), and those of IC 342 Source 1 in Okada et al. (1998), Mizuno et al. (1999), Watarai, Mizuno and Mineshige (2001) and Kubota et al. (2001).

We assume the diluted blackbody local spectra with  $T_{col}/T_{eff} = 1.7$  in sections 3.1 and 3.2. Difference among the Newtonian, Schwarzschild, and Kerr disk models are only the relativistic effects, including the variation of the innermost radius and energy conversion efficiency (appendix A). The Schwarzschild disk model we use (GRAD model) is explained in Hanawa (1989) and Ebisawa, Mitsuda and Hanawa (1991) (see also appendix B). The GRAD model is available in the XSPEC spectral fitting package, and this model also provides the Newtonian disk spectra, when the relativistic switch is turned off.

#### 3.1. Application to GRO J1655–40

In Table 1, we show results of spectral fitting of the ASCA GIS spectra with Newtonian, Schwarzschild, and extreme Kerr disk models. System parameters have been determined from optical observations (Orosz and Bailyn 1997), such that distance is 3.2 kpc, inclination angle is  $70^\circ$ , and  $M = 7M_\odot$ . We fixed the distance, while several different inclination angles are tried from  $0^\circ$  to  $80^\circ$ . The energy spectrum has a power-law hard-tail but contribution of which is minor below 10 keV and hardly affects discussion of the accretion disk spectrum. The power-law slope is fixed at 2.5 which matches the simultaneous high energy observation with BATSE (Zhang et al. 1997), and its normalization is allowed to be free within the range acceptable by BATSE. Hence, the free parameters are  $M$ ,  $\dot{M}$ , power-law normalization, and the hydrogen column density. Besides minor local features (see Gieliński, Maciolek-Niedzwiecki and Ebisawa 2001), all the models with different inclination angles can reasonably fit the observed accretion disk spectrum.

Note that the Schwarzschild disk model at the correct inclination angle ( $i = 70^\circ$ ) gives a too small mass ( $1.8M_\odot$ ) which is unacceptable (red curve in Figure 3 left). If we fix the mass at the correct value ( $7M_\odot$ ), the disk spectrum cannot be hard enough to explain the observed spectrum (the “best-fit” is shown with green curve in Figure 3 left): The “too-hot” disk problem is evident (equation 2).

It is of interest to see how the black hole mass depends on the inclination angle. Observation can constrain the projected disk area, which is proportional to square of the mass. Hence  $M \propto 1/\sqrt{\cos i}$  in the Newtonian case, and the black hole mass at  $i = 80^\circ$  is 2.4 times higher than that for the face-on disk. On the other hand, the mass increasing factor is 2.9 in the Schwarzschild case, and as much as  $\sim 10$  in the extreme Kerr case. This is because inclined relativistic disk spectra become harder, which is most conspicuous in the extreme Kerr disk (section 2.4; figure 1). Given the observed spectra, to compensate the spectral hardening with inclination, the mass becomes necessarily larger (equation 2).

The extreme ( $a=0.998$ ) Kerr disk model with the correct inclination angle gives  $M = 15.9M_\odot$ . Compared to the fit with Schwarzschild disk model ( $1.8M_\odot$ ), significant increase of the mass does indicate the spectral hardening of the Kerr disk model. In fact, the derived mass is too large to be consistent with the realistic mass  $7 M_\odot$ , which probably suggests that  $a=0.998$  is too high. In fact, Gielinski, Maciolek-Niedzwieck and Ebisawa (2001) applied the Kerr disk model to the same ASCA energy spectrum of GRO J1655-40, and concluded that  $a$  is likely to be between 0.68 and 0.88 to be consistent with  $M = 7M_\odot$ . To summarize, in agreement with Gielinski, Maciolek-Niedzwieck and Ebisawa (2001), a standard Kerr disk model may explain the observed accretion disk spectra of GRO J1655-40 at the inclination angle  $i = 70^\circ$ . The Kerr metric is required, but not with the maximum angular momentum.

Probability that GRO J1655-40 has a spinning black hole is also suggested by the recent discovery of 450 Hz QPO (Strohmayer 2001), as this frequency is higher than the Kepler frequency at the innermost stable orbit of a  $7 M_\odot$  Schwarzschild black hole. Precise analysis of the QPO characteristics from GRO J1655-40 suggests that the black hole is in neither a Schwarzschild nor a maximal Kerr black hole (Abramowicz and Kluźniak 2001), which is consistent with our energy spectral analysis.

### 3.2. Application to IC342 Source 1

We assume the distance to the source 4 Mpc (Okada et al. 1998 and references there in). If isotropic emission is assumed, the luminosity will be  $1.7 \times 10^{40}$  erg s<sup>-1</sup> (1 - 10 keV) at this distance, thus  $M \gtrsim 100M_\odot$  is expected so as not to exceed the Eddington luminosity. In table 2, we summarize results of the spectral fitting of the ASCA GIS spectrum with Newtonian, Schwarzschild, and Kerr disk models, for different inclination angles. All the fits are acceptable, thus models may not be discriminated based on the fitness for the observation. Note that the disk luminosities always exceed the Eddington limit more than 10 times in the Schwarzschild case.

The right panel in figure 3 indicates the ASCA GIS spectrum and the best-fit Schwarzschild disk model (in red). For comparison, we show a Schwarzschild disk spectrum with  $M = 100M_{\odot}$  at the Eddington limit (in green). We can clearly see that such an accretion disk has a too low temperature to explain the observed hard spectrum.

The face-on Kerr disk model gives  $M = 27.3M_{\odot}$  and  $\dot{M} = 2.0 \times 10^{20} \text{ g s}^{-1}$  ( $\dot{M} = 16 \dot{M}_C$ ). A factor of  $\sim 3$  increase of the mass compared to the Schwarzschild case is due to slight hardening of the face-on Kerr disk spectrum. Note that *the super-Eddington problem does not disappear*, as the face-on Kerr disk spectrum is not very different from the Schwarzschild one (section 2.4; figure 1). If we assume a very inclined disk with  $i = 80^\circ$ , we obtain  $M = 332M_{\odot}$  and  $\dot{M} = 1.5 \times 10^{20} \text{ g s}^{-1}$  ( $\dot{M} = 1.0 \dot{M}_C$ ). Now the super-Eddington problem is solved, that is consequence of the fact that the inclined Kerr disk spectrum is much harder than the Schwarzschild one. However, there will be two serious problems to accept the inclined Kerr disk model for ULXs in general: First, we do not know a mechanism to create  $\sim 350M_{\odot}$  black holes. Second, it is very unlikely that most of the accretion disks in ULXs are largely inclined when seen from the earth.

### 3.3. Examination of Variants of Standard Disk Model

In this section, we critically examine two possibilities which have been proposed to make the standard accretion disk spectra look harder.

#### 3.3.1. Large $T_{col}/T_{eff}$ ?

A naive solution to explain the apparently hard disk spectrum may be to allow  $T_{col}/T_{eff}$  to be much greater than the standard value  $\sim 1.7$ , in which case the color temperature of the disk can be much higher for the same mass and mass accretion rate, while the effective temperature remains the same (equation 2). In other words, for a given observed disk flux and spectrum,  $M \propto (T_{col}/T_{eff})^2$ , thus a larger mass is allowed (equation 3).

In fact, in the case of GRO J1655-40, (Section 3.1, table 1), if  $T_{col}/T_{eff} = 1.7\sqrt{7M_{\odot}/1.8M_{\odot}} = 3.4$ , the observed spectrum is explained with the Schwarzschild disk model with  $7M_{\odot}$  for the same distance and inclination angle. Borozdin et al. (1998) reached a similar conclusion that  $T_{col}/T_{eff} = 2.6$  is required for GRO J1655-40 to fit with a Newtonian disk model whose inner disk radius is 3 times the Schwarzschild radius. For IC342 Source 1, we need a still higher value of  $T_{col}/T_{eff} = 1.7\sqrt{100M_{\odot}/8.9M_{\odot}} = 5.7$ , to fit with a face-on Schwarzschild disk model around a  $100M_{\odot}$  black hole.

Although having high  $T_{col}/T_{eff}$  values might seem to solve the “too-hot” disk problem,  $T_{col}/T_{eff} \gtrsim 2$  for Galactic sources and ULXs is most certainly excluded both from theory and observation. Independent theoretical calculations agree with values of  $T_{col}/T_{eff} = 1.7 - 1.9$  for accretion disks around  $\sim 10M_{\odot}$  black hole (Shimura and Takahara 1995; Ross and Fabian 1996; Blaes et al. 2001). Values of  $T_{col}/T_{eff}$  increase very slowly with mass, but cannot be higher than  $\sim 2.5$  even for a  $10^6M_{\odot}$  black hole (Ross, Fabian and Mineshige 1992; Blaes et al. 2001). From observations, when applied to accretion disk spectra of Galactic black hole candidates or weakly magnetized neutron stars,  $T_{col}/T_{eff} = 1.7 - 1.9$  gives reasonable mass values which are consistent with those derived from more reliable methods (e.g., Ebisawa, Mitsuda and Hanawa 1991; Ebisawa et al. 1993; Shimura and Takahara 1995; Dotani et al. 1997). If we happen to use  $T_{col}/T_{eff} \approx 2.6$  for an accretion disk around a weakly magnetized neutron star, the neutron star mass exceeds  $\sim 3M_{\odot}$ , which is not acceptable.

### 3.3.2. Comptonization of disk photon?

If a standard optically thick disk is shrouded by a thermal corona whose temperature is slightly higher than the disk temperature, significant parts of the disk photons are comptonized and appear in higher energy bands. Thus, in such a situation, the observed hard energy spectra from Galactic superluminal jet sources and ULXs might be explained.

The comptonization model may phenomenologically fit the observed spectra of GRO J1655-40 (Zhang et al. 2000; Życki, Done and Smith 2001). Fitting with a thermal comptonization model (in which seed photons have a single temperature black body spectrum) gives typically the black body temperate  $\lesssim 0.5$  keV, plasma temperature  $\sim 1.5$  keV and scattering optical depth  $\sim 10$ . At such a low temperature and high optical depth, the heavy elements may not be fully ionized, and the plasma can be optically thick to photoelectric absorption. Presumably, such a physical situation is more reasonably described by standard optically thick accretion disk in which emergent spectrum is distorted by Comptonization ( $T_{col} > T_{eff}$ ), which successfully explain the observation (section 3.1).

We applied the comptonization model to IC342 Source 1. When the seed photon is assumed to be disk blackbody, we obtain  $T_{in} \approx 1.2$  keV, plasma temperature  $\sim 2.5$  keV, and scattering optical depth  $\sim 10$  ( $\chi^2/\text{dof}=51.8/46$ ). Note that the  $T_{in}$  cannot go down to  $\sim 0.7$  keV as desired for the Schwarzschild disk around a  $100 M_{\odot}$  black hole. Therefore, the original “too-hot” disk problem may not be solved even introducing the ad hoc comptonization plasma to harden the standard disk spectrum. When the seed photon spectrum is assumed to be black body, the black body temperature is 0.52 keV, the plasma temperature is 1.8 keV and the optical depth is  $\sim 18$  ( $\chi^2/\text{dof}=51.8/46$ ). Although this model may fit the data,

it is hard to interpret these parameters in the physical context, and the super-Eddington problem is unanswered. Presumably, the slim disk model explained in the next section is more likely for ULXs.

## 4. The Slim Disk Model

### 4.1. Characteristics of the slim disk model

So far, we have considered the standard optically thick accretion disk (Shakura and Sunyaev 1973) in which radial energy advection is neglected and all the gravitational energy release is converted to thermal radiation. In accretion disk theory (for a review, e.g., Kato, Fukue and Mineshige 1998), there is another stable optically thick solution, which is called “optically thick ADAF (advection-dominated accretion flow)” disk or, “slim” disk (Abramowicz et al. 1988), which takes place when mass accretion rate is extremely high. In the slim disk, all the gravitational energy release is not converted to the thermal radiation, but significant part of the energy is carried inward due to radial advection. Slim disk is geometrically thick, and can be much hotter than the standard disk (Kato, Fukue and Mineshige 1998; Watarai et al. 2000).

One of the most significant observational characteristics of the slim disk is that the disk luminosity can exceed the Eddington limit by up to  $\sim 10$  times (Abramowicz et al. 1988; Szuszkiewicz, Malkan and Abramowicz 1996; Kato, Fukue and Mineshige 1998). This may be qualitatively understood as follows: At any disk radius, local radiation pressure may not exceed the vertical gravitational force, such that

$$F(r) \lesssim \frac{cGM}{\kappa r^2} \frac{h}{r}, \quad (4)$$

where  $F(r)$  is the energy flux,  $r$  the disk radius and  $h$  the half-thickness. Therefore,

$$\begin{aligned} L_{disk} &\equiv 2 \int_{r_{in}}^{r_{out}} 2\pi r F(r) dr \\ &\lesssim \frac{4\pi cGM}{\kappa} \int_{r_{in}}^{r_{out}} \frac{h}{r^2} dr \\ &\approx L_{Edd} \left( \frac{h}{r} \right) \ln \left( \frac{r_{out}}{r_{in}} \right), \end{aligned} \quad (5)$$

where  $r_{in}$  and  $r_{out}$  are inner and outer disk radius, respectively, such that  $\ln(r_{out}/r_{in}) \approx 10$ . In the standard disk, which is geometrically thin,  $h/r \lesssim 0.1$ , thereby  $L_{disk} \lesssim L_{Edd}$ . On the other hand, with the slim disk in which  $h/r \approx 1$ ,  $L_{disk} \lesssim 10 L_{Edd}$ .

In addition to that super-Eddington luminosities are permissible, slim disk has following observational characteristics (e.g., Kato, Fukue and Mineshige 1998; Watarai et al. 2000; Watarai, Mizuno and Mineshige 2001): (1) As the mass accretion rate exceeds the critical rate  $\dot{M}_C$ , energy conversion efficiency decreases due to advection (appendix A, figure 7). Hence the disk luminosity is no longer proportional to the mass accretion rate, but saturates at  $\sim 10 L_{Edd}$ . (2) Innermost disk radius can be closer to the black hole than the last stable orbit, as mass accretion rate increases. Even in the Schwarzschild metric, innermost disk region inside  $6 r_g$  can emit significant amount of X-rays. Thus slim disk can be “hotter” than the standard disk. (3) If radial dependence of the disk effective temperature is written as  $T_{eff} \propto r^{-p}$  (“ $p$ -free disk” below), the exponent  $p$  reduces from 0.75 (which is expected for the standard disk) to 0.5 as advection progressively dominates. Thus spectral difference from the standard disk will be noticeable.

#### 4.2. Slim disk for Galactic Sources?

Watarai et al. (2000) suggested that the slim disk model may explain the apparently hard energy spectra of Galactic superluminal jet sources. In fact, energy spectra of GRO J1655–40 (Kubota 2001), GRS 1915+105 (Yamaoka 2001) and XTE J1550-56 (Kubota 2001) are not fitted with a standard accretion disk model when their disk luminosities and temperatures reached maxima, but better fitted with the  $p$ -free disk model with  $p$  between 0.75 and 0.5. This is considered to be an evidence of emergence of the slim disk, when mass accretion rates are extremely high in these sources.

On the other hand, when the disk luminosity and temperature are lower, GRO J1655–40 is considered to embrace the standard disk, since the standard disk model can fit the observed spectra well, and the inner disk radius is fairly constant over a large luminosity variation (Sobczak et al. 1999; Kubota, Makishima and Ebisawa 2001). Without advection, the standard Kerr disk with high inclination is successful to explain the observed hard disk spectra (section 3.1). Therefore, except when the disk luminosity is near the peak and the slim disk presumably takes place, the standard disk is expected to be present in the Galactic superluminal jet sources.

#### 4.3. Application to IC342 Source 1

As for ULXs, the slim disk model seems to be more likely, as ULXs are intrinsically bright systems. Mizuno, Kubota and Makishima (2001) studied spectral variations of several ULXs,

and commonly found anti-correlation between the MCD parameters  $R_{in}$  and  $T_{in}$ , which is another observational feature of the slim disk (Watarai et al. 2000). Watarai, Mizuno and Mineshige (2001) calculated energy spectra of slim disks around intermediate mass black holes, and suggested that ULXs are slim disks around  $10 - 30 M_{\odot}$  black holes shining more luminously than Eddington limits.

In the present paper, we fit the observed energy spectra with the same slim disk model calculated by Watarai, Mizuno and Mineshige (2001). Namely,  $\alpha = 0.01$ , and the local emission is a diluted blackbody with  $T_{col}/T_{eff} = 1.7$ . The model assumes the face-on geometry, and the distance is 4 Mpc. The energy spectra are calculated for each grid point of  $M = 10, 32, 100 M_{\odot}$  and  $\dot{M}/(L_{Edd}/c^2) = 1, 3, 10, 32, 100, 320, 1000$ . We fitted the observed spectra using XSPEC spectral fitting package with this grid-model, so that XSPEC interpolates the model spectra for other  $M$  and  $\dot{M}$  values.

Fitting result for IC342 Source 1 ASCA GIS spectrum is shown in table 3. We find  $M = 19.8M_{\odot}$  and  $\dot{M}/\dot{M}_C \approx 20$ . This mass accretion rate would give 20 times the Eddington luminosity in the case of the standard disk. However, since slim disk is less efficient at  $\dot{M} \gtrsim \dot{M}_C$  (appendix A and figure 7), the disk luminosity is in fact only  $\sim 6$  times the Eddington luminosity, which is allowed in the slim disk (section 4.2).

The slim disk model can fit the observed spectra reasonably well ( $\chi^2/\text{dof} = 1.40$ ), but not as good as the standard disk models ( $\chi^2/\text{dof} \approx 0.90$ ; table 2) (figure 4). Also, the hydrogen column density is significantly larger with the slim disk model ( $\sim 9 \times 10^{21} \text{ cm}^{-2}$ ) compared to those with the standard disk models ( $3-5 \times 10^{21} \text{ cm}^{-2}$ ). This is because the spectral difference between the best-fit slim disk model and standard disk spectra is largest in the lower energy band (figure 5). We simply assumed diluted blackbody local spectra with constant  $T_{col}/T_{eff}$ , which is known to be a good approximation for the standard disk (section 2.3). However, precise theoretical calculation of the local spectrum in the slim does not exist yet, and more realistic slim disk spectral model is expected to fit the observed spectra better.

#### 4.4. Spectral Variation of IC342 Source 1

The characteristic anti-correlation between  $R_{in}$  and  $T_{in}$  discovered by Mizuno, Kubota and Makishima (2001) is considered to be a characteristic of the slim disk. Watarai, Mizuno and Mineshige (2001), through indirect comparison of the MCD parameters and slim disk spectra, claimed that this spectral variation may be explained with a slim disk a constant  $M$  only by varying the mass accretion rate. We demonstrate this claim by directly fitting

the ASCA IC 342 Source 1 spectra with the slim disk model.

We use the same spectral datasets used by Mizuno, Kubota and Makishima (2001). The observation period is split into five periods depending on the flux levels. For each period, GIS and SIS spectra are fitted simultaneously to achieve the better statistics. In the top panel of figure 6, we show  $M$  and  $\dot{M}$  variation obtained with the face-on GRAD model. We fixed the hydrogen column density at the average value ( $N_H = 5.2 \times 10^{21} \text{cm}^{-2}$ ), so that the free parameters are only  $M$  and  $\dot{M}$ . We see clear anti-correlation between these two parameters, which is just rephrasing the  $R_{in}-T_{in}$  anti-correlation discovered by Mizuno, Kubota and Makishima (2001). Since  $M$  should not vary in reality, this relation is telling that the standard accretion disk is not a proper model for IC 342 Source 1. The spectral variation is clearly seen using only the 2 – 10 keV band, though less clear than using the entire 0.5 – 10 keV band.

Since the present slim disk model does not fit the observed spectra well below  $\sim 1.5$  keV, we study spectral variation only using 2 – 10 keV. For fair comparison, the hydrogen column density was fixed to the same average value as used in the GRAD model fitting. The  $M$  and  $\dot{M}$  relation obtained from the slim disk fitting is shown in the bottom panel in figure 6. We see that  $M$  in the range of  $22.5 M_\odot$  to  $23.9 M_\odot$  is consistent with all the five spectra. Therefore, on the slim disk model, we may interpret the observed spectral variation of IC 342 Source 1 as a result of simple mass accretion rate changes.

#### 4.5. Future Problems of the Slim Disk Model

Compared to the standard disk model, X-ray spectral study from the slim disk has only a short history. As already stated above, the present slim disk model may not fit the observed ASCA spectra perfectly well, though the spectral variation is correctly described. However, there are several problems to calculate the slim disk spectra precisely, and this is not an easy problem. Although the face-on geometry is assumed in the present slim disk model, observed flux from a slim disk is considered to be strongly inclination angle dependent. The flux drops with inclination angle  $i$  more rapidly than  $\cos i$ , because the horizontal photon diffusion time-scale gets longer than the in-fall time-scale (Kato, Fukue and Mineshige 1998). Also, if the slim disk exists around a Kerr black hole, the disk can be much hotter than the Schwarzschild case (Beloborodov 1998). In addition, effects of radial photon-trapping may not be negligible under extremely high accretion rates (Ohsuga et al. 2002), by which  $T_{col}/T_{eff}$  may have a significant radial dependence (Shimura and Manmoto 2003). More precise spectral model calculation from the slim disk is anticipated overcoming these difficulties.

## 5. Origin of the Ultra-Luminous X-ray Sources

We have shown that the slim disk model is likely to explain the observed super-Eddington luminosities, hard energy spectra, and spectral variations of IC342 Source 1. From the spectral fitting, we obtained the black hole mass  $\sim 20M_{\odot}$ , and the disk luminosity  $\sim 6$  times the Eddington luminosity. Thus, “intermediate mass black holes” are not required to explain the observed luminosity  $\sim 10^{40}$  erg s $^{-1}$ .

In our Galaxy, the most massive stellar black hole is  $\sim 14M_{\odot}$  in GRS 1915+40 (Greiner, Cuby and McCaughrean 2001), as far as currently measured. However, more massive stellar black holes may well exist in other galaxies, since stellar evolution theory says main-sequence stars can have a maximum mass  $\sim 60M_{\odot}$  (Schwarzschild and Härm 1959). Grimm, Gilfanov and Sunyaev (2003) claims that there exists a universal luminosity function of the high mass X-ray binaries, such that the normalization is determined by the star-forming rate. Galaxies which are active in star formation tend to have more luminous and massive compact objects, and the maximum cut-off luminosity is  $\sim 10^{40}$  erg s $^{-1}$ . It is likely that ULXs with luminosities of  $\sim 10^{40}$  erg s $^{-1}$  are stellar mass black holes having a few tens of solar mass, which reside at the brightest end of the luminosity function.

## 6. Conclusion

1. In order to solve the “too-hot disk” problem of ULXs and Galactic superluminal jet sources, we have carefully studied energy spectra of standard accretion disk and slim disk. In particular, we have calculated the extreme Kerr disk spectral model, and studied how relativistic effects and disk inclination angle affect the observed disk spectra.
2. We have found that the Kerr disk model can successfully explain the observe hard spectra of GRO J1655–40, because the Kerr disk spectra become significantly harder than Schwarzschild ones when the disk is significantly inclined, that is the case for GRO J1655-40.
3. The Kerr disk spectra are not significantly harder than the Schwarzschild disk when disk inclination angle is not large. We conclude that the standard Kerr disk model is not appropriate to explain the observed hard spectra of ULXs, as it is unlikely that accretion disks in most ULXs are preferentially inclined, and, if the inclined Kerr disk is applied, unreasonably large black hole mass ( $\sim 300M_{\odot}$ ) is required.
4. We have calculated the slim disk spectra, and applied to the observed spectra of IC342 Source 1. Although the current primitive slim disk model does not perfectly fit the

data, we found the slim disk can explain the observed super-Eddington luminosity, hard X-ray spectra, and spectral variation. In particular, the characteristic spectral variation is explained with constant mass at  $M \sim 20M_{\odot}$  with simple mass accretion rate variation.

5. We propose ULXs are a few tens of solar mass black holes, which reside at the bright end of the X-ray binary luminosity function.

We are grateful to Prof. K. Makishima for useful comments and discussion. We are thankful to Drs. D. Bhattacharya, S. Bhattacharya and A. V. Thampan for finding bugs in the old GRAD code, and comparing the fixed GRAD code with their accretion disk model. We are glad to Dr. Hanawa for developing the original GRAD code and fixing the bugs. We acknowledge Dr. A. Laor for making his transfer function calculation available with the XSPEC package. This research has made use of public data and software obtained from the High Energy Astrophysics Science Archive Research Center (HEASARC), provided by NASA's Goddard Space Flight Center. This work was supported in part by Polish KBN grant 2P03D01718.

### A. Energy Conversion Efficiency and Critical Mass Accretion Rates

Energy conversion efficiency of optically thick accretion disk ( $\eta$ ) is dependent on disk model assumptions, so that a particular care is needed to interpret the disk parameters we obtain from spectral model fitting. In particular, conversion efficiency of the slim disk model is dependent on the mass and mass accretion rates (Watarai et al. 2000; Watarai, Mizuno and Mineshige 2001).

In the Newtonian case, energy loss in the standard disk per second ( $\equiv$  disk luminosity,  $L_{disk}$ ) may be written as

$$\begin{aligned} L_{disk} &= \dot{M} \left( \frac{GM}{r_{in}} - \frac{L^2}{2r_{in}^2} \right) \\ &= \frac{GM\dot{M}}{2r_{in}}, \end{aligned}$$

where  $r_{in}$  is the innermost radius, and  $L$  is the specific angular momentum at  $r_{in}$ ,  $\sqrt{GM r_{in}}$ . If we take  $r_{in}$  as the last stable orbit in the Schwarzschild metric,  $6 r_g = 6 GM/c^2$ ,  $L_{disk} = \frac{1}{12} \dot{M} c^2$ , hence  $\eta = 1/12$  for the Newtonian disk. In the Pseudo-Newtonian potential, which

the present slim disk model adopts,

$$L_{disk} = \dot{M} \left( \frac{GM}{r_{in} - 2r_g} - \frac{L^2}{2r_{in}^2} \right),$$

where  $L = \sqrt{GM r_{in}^3 / (r_{in} - 2r_g)^2}$ . With  $r_{in} = 6 r_g$ , we obtain  $\eta=1/16$ . This is close enough to the correct efficiency in the Schwarzschild metric,  $\eta=0.057$ . For the extreme Kerr case with  $a = 0.998$  and  $r_{in} = 1.24 r_g$ ,  $\eta = 0.366$ .

We may define the critical accretion rate  $\dot{M}_C$  so that  $L_{Edd} \equiv \eta \dot{M}_C c^2$ , where  $L_{Edd}$  is the Eddington luminosity. For the Schwarzschild case with  $r_{in} = 6 r_g$ ,  $\dot{M}_C = 2.9 \times 10^{18} (M/M_\odot) \text{ g s}^{-1}$ , and for the Newtonian case with the same innermost radius,  $\dot{M}_C = 2.0 \times 10^{18} (M/M_\odot) \text{ g s}^{-1}$ . For the extreme Kerr case  $\dot{M}_C = 4.6 \times 10^{17} (M/M_\odot) \text{ g s}^{-1}$ .

In the pseudo-Newtonian potential, if the innermost radius is constant at  $r_{in} = 6 r_g$ ,  $\dot{M}_C = 2.7 \times 10^{18} (M/M_\odot) \text{ g s}^{-1}$ . However, in the present slim disk model, the inner radius becomes smaller than  $6 r_g$ , and the energy advection is dominant at high accretion rates (Watarai et al. 2000). Hence, the conversion efficiency is dependent on the mass and mass accretion rate. In figure 7, we show conversion efficiency of the slim disk for several mass and mass accretion rate values. We see that at low mass accretion rate limits,  $\eta \approx 1/16$ , but the efficiency significantly decreases with mass accretion rates when  $\dot{M} \gtrsim \dot{M}_C$  due to the advection effect.

## B. Bugs in the original GRAD model

Three mistakes have been found in the appendix of Ebisawa, Mitsuda and Hanawa (1991; EMH) besides obvious typos:

- (A8) in EMH should be read as follows:

$$\frac{d\theta'_{ph}}{d\theta_{ph}} = \frac{\cos i \sin \theta_{ph} + \sin i \cos \theta_{ph} \sin \varphi_{ph}}{\sin \theta'_{ph}}. \quad (\text{B1})$$

- (A15) in EMH should be read as follows:

$$\frac{\epsilon_{DO}}{\epsilon_{LO}} = \sqrt{1 - \frac{3GM}{rc^2}} \left[ 1 - \left( 1 - \frac{2GM}{rc^2} \right)^{-0.5} \sqrt{\frac{GM}{rc^2}} \frac{r}{c} \frac{d\varphi'_{ph}}{dt_{ph}} \right]^{-1}. \quad (\text{B2})$$

The bold-face part was 1 in EMH, which is wrong.

- (A22) in EMH should be read as follows:

$$T_{\text{col}} = 1.11 \left( \frac{T_{\text{col}}/T_{\text{eff}}}{1.5} \right) \left[ \frac{g(r/r_g)}{0.15} \right] \left( \frac{M}{1.0 M_{\odot}} \right)^{-1/2} \left( \frac{\dot{M}}{10^{18} \text{ g s}^{-1}} \right)^{1/4} \text{ keV.} \quad (\text{B3})$$

The bold-face part was 1.4 in EMH, which is incorrect.

Below, equations (A1) to (A4) refer to those in the present appendix, not in EMH. Equation (B1) was already fixed in the GRAD model code used in EMH, which was distributed with XSPEC version 11.0.1ae and previous ones. Equations (B2) and (B3) were *not* fixed in the code, and the wrong values were used in EMH. In addition, there was another bug in the code used in EMH: In the part to calculate the disk flux,

$$F = 8.9038633D - 3 * F/\text{Ratio} * *4/(D/10.0) * *2 * (\text{Em}/1.4) * *2$$

was wrong, and this has to be

$$F = 8.9038633D - 3 * F/\text{Ratio} * *4/(D/10.0) * *2 * \mathbf{Em} * *2, \quad (\text{B4})$$

where Em denotes the compact object mass. These bugs in equation (B3) and (B4) compensate each other (but not perfectly), which probably explains why we could not notice these bugs much earlier. The bug in equation (B2) affects only when the disk is inclined, and this effect is not significant.

Besides the bug in equation (B2), one can see from equations (B3) and (B4) that the old GRAD spectra with  $M = 1.4M_{\odot}$  and the new GRAD spectra with  $M = 1.0M_{\odot}$  are identical. Therefore, besides the minor difference of redshifts which originates in (B2), when an observed spectrum was fitted with the old GRAD model, *the mass of the compact object was erroneously 1.4 times higher than the correct mass given by the fixed GRAD model*. This should be taken into account to interpret published results obtained using the old GRAD model (e.g., Ebisawa, Mitsuda and Hanawa 1991; Kitamoto, Tsunemi and Roussel-Dupre 1992; Ebisawa et al. 1993; Dotani et al. 1997; Kubota et al. 1998). The mass accretion rate represented in the dimension of mass per time is unchanged. The fixed GRAD code is distributed with XSPEC version 11.1.0 and on.

Note that the bug in the old GRAD code may compensate with an ambiguity of  $T_{\text{col}}/T_{\text{eff}}$  values. In fact, in Ebisawa, Mitsuda and Hanawa (1991) and Ebisawa et al. (1993), we used  $T_{\text{col}}/T_{\text{eff}} = 1.5$  and obtained reasonable masses of black holes and neutron stars, which should be reduced by 1.4 times using the correct GRAD model. On the other hand, the mass estimate is proportional to  $(T_{\text{col}}/T_{\text{eff}})^2$  (when distance is known) or  $(T_{\text{col}}/T_{\text{eff}})^4$  (when  $d/\sqrt{M}$  is known), thus using  $T_{\text{col}}/T_{\text{eff}} = 1.8$  or 1.6 instead of 1.5 retrieves the original mass

values. The higher  $T_{col}/T_{eff}$  values are in fact consistent with a precise calculation carried out more recently (Shimura and Takahara 1995; Ross and Fabian 1996).

We confirmed that the fixed GRAD model gives almost identical spectra with the Schwarzschild disk spectra calculated by Bhattacharyya, Bhattacharya and Thampan (2001). Only a minor difference is found when the accretion disk is more inclined than  $\sim 60^\circ$ , when the model by Bhattacharyya, Bhattacharya and Thampan (2001) gives as much as  $\sim 10\%$  higher flux at  $\sim 10$  keV. The discrepancy is probably due to the fact that the GRAD model does not take account of the photons whose trajectories change directions more than 180 degrees. In fact, those photons may not be observable being blocked by the putative plasma near the black hole which is responsible for generation of the power-law hard-tail component.

### C. Comparison of Newtonian and Schwarzschild Accretion Disk Spectra

Comparison of the GRAD and MCD model parameters have been made by EMH, which is affected by the bug explained above. Here, we present correct results using the new GRAD code after the bug is fixed. Also, we discuss how the relativistic effects (in the Schwarzschild case) affect the mass and mass accretion rate determination from observed accretion disk spectra.

MCD model does not take into account the inner boundary condition, but simply assumes  $T(r) = T_{in} (R_{in}/r)^{3/4}$ , where  $R_{in}$  and  $T_{in}$  are the *apparent* inner disk radius and temperature, respectively. MCD model is useful to represent observed spectra, since it has the two independent parameters which are directly constrained from observation, such that the spectral shape is determined only by  $T_{in}$ , and the normalization is proportional to  $R_{in}^2 \cos i$ , where  $i$  is the inclination. Often disk inclination is unknown, so that  $R_{in}$  is uncertain and proportional to  $(\cos i)^{-0.5}$ .

Relationship between the MCD  $T_{in}$  and  $R_{in}$  parameters and the mass and mass accretion rate in the Newtonian disk model with correct boundary condition is given as (see also Kubota et al. 1998),

$$M \approx 0.05 \left( \frac{T_{col}}{T_{eff}} \right)^2 (R_{in} \text{ km}) M_\odot, \quad (\text{C1})$$

$$T_{in} \approx 1.1 \left( \frac{T_{col}}{T_{eff}} \right) \left( \frac{\dot{M}}{10^{18} \text{ g s}^{-1}} \right)^{1/4} \left( \frac{M}{M_\odot} \right)^{-1/2} \text{ keV}. \quad (\text{C2})$$

The multicolor disk spectrum and the Newtonian disk with correct boundary condition have almost identical spectral shape in 0.5 - 15 keV when equations (C1) and (C2) are

considered.

Formulae to relate the new GRAD model parameters and MCD parameters are the following:

$$M \approx \begin{pmatrix} 0.031 \\ 0.039 \\ 0.045 \\ 0.050 \\ 0.048 \end{pmatrix} \left( \frac{T_{col}}{T_{eff}} \right)^2 (R_{in} \text{ km}) M_{\odot} \text{ for } i = \begin{pmatrix} 0^{\circ} \\ 30^{\circ} \\ 45^{\circ} \\ 60^{\circ} \\ 80^{\circ} \end{pmatrix}, \quad (\text{C3})$$

$$T_{in} \approx \begin{pmatrix} 0.75 \\ 0.80 \\ 0.85 \\ 0.92 \\ 0.96 \end{pmatrix} \left( \frac{T_{col}}{T_{eff}} \right) \left( \frac{\dot{M}}{10^{18} \text{ g s}^{-1}} \right)^{1/4} \left( \frac{M}{M_{\odot}} \right)^{-1/2} \text{ keV for } i = \begin{pmatrix} 0^{\circ} \\ 30^{\circ} \\ 45^{\circ} \\ 60^{\circ} \\ 80^{\circ} \end{pmatrix}. \quad (\text{C4})$$

The numerical coefficients have been obtained by fitting the new GRAD spectra with multicolor disk model (see below)<sup>3</sup>.

In Figure 8, we illustrate the relationship of the MCD model parameters and  $M$  and  $\dot{M}$  in the Newtonian and GRAD models. These figures are made by simulating GRAD and Newtonian model spectra with various values of mass, mass accretion rate and inclination, using the *Ginga* response (sensitive in 1 – 30 keV), assuming the distance 1 kpc and exposure time 3000 sec exposure. These simulated spectra are fitted with the MCD model, and the best-fit  $R_{in}$  and  $T_{in}$  are obtained.

From equations (C1) to (C4) and Figure 8, for a given observed spectrum for which  $R_{in}$  and  $T_{in}$  are determined, we can see the following (see also Table 2 and 1):

- When fitting the same observed spectra, we will get a smaller mass and higher accretion rate with the GRAD model than with the Newtonian disk.
- Differences in the mass and mass accretion rate between the GRAD model and the Newtonian models are the largest for the face-on disk, and get smaller with inclination.

These characteristics of the GRAD model are due to relativistic effects, and may be understood intuitively as follows. Because the conversion efficiency of the GRAD model (0.057) is smaller than that of the Newtonian disk (0.083), the GRAD model requires a

---

<sup>3</sup>Equations (3) in Ebisawa, Mitsuda and Hanawa (1991) was wrong such that the old formula gives 1.4 times larger mass for the same  $R_{in}$  and  $T_{in}$ .

higher mass accretion rate to shine with the same luminosity. Thus we need a higher mass accretion rate with the GRAD model when fitting the same observed spectra. The observed disk flux is proportional to  $L_{disk} \cos i$ , thus the disk luminosity induced from the observed flux is  $L_{disk} \propto (\cos i)^{-1}$ . Consequently, the mass accretion rate is proportional to  $(\cos i)^{-1}$  in the Newtonian case. In the GRAD model, this dependence becomes milder, because the face-on disk tends to be dimmer due to the light bending effect in the vicinity of the black hole, while those photons removed from the near face-on disks turn out to be the flux enhancement for the inclined disks. In fact, for the face-on disk, the GRAD mass accretion rate is  $\sim 1.8$  time larger than that of the Newtonian disk, whereas it is  $\sim 1.1$  times for  $i = 80^\circ$ .

Because of the gravitational redshift, the GRAD model gives a smaller characteristic disk temperature than the Newtonian disk with the same mass and mass accretion rate (compare equations C2 and C4). To achieve the same characteristic disk temperature of the Newtonian model, the  $\sim 1.8$  times mass accretion rate increase is not sufficient, and the mass has to get smaller too. Since we measure the projected disk area  $\propto M^2 \cos i$ , the mass increases with inclination as  $(\cos i)^{-0.5}$  in the Newtonian case, while the GRAD disk temperature gets higher because of the Doppler boost. Therefore, ratio of the GRAD mass to the Newtonian mass is the smallest for the face-on disk ( $\sim 0.6$ ) and gets larger with inclination ( $\sim 0.73$  for  $i \gtrsim 60^\circ$ ).

It is interesting that difference of the Newtonian and GRAD model parameters are the largest for the face-on disk and the smallest for highly inclined disks where relativistic effects are supposed to be most significant. This is because the gravitational redshift and Doppler boosts more or less cancel each other for a highly inclined Schwarzschild disk. This is in contrast to the extreme Kerr disk, where near edge-on disks show extremely hard spectra due to enormous Doppler boosts (see figure 1 and 2).

## REFERENCES

- Abramowicz, M. A., Czerny, B., Lasota, J.-P. and Szuszkiewicz, E. 1988, ApJ, 332, 646
- Abramowicz, M. A. and Kluźniak, W. 2001, A&A, 374, L19
- Asaoka, I. 1989, PASJ, 41, 763
- Bauer F. E. et al. 2001, AJ, 122, 182
- Bhattacharyya, S. Bhattacharya, D. and Thampan, A. V. 2001, MNRAS, 325, 989
- Belloni, T. et al. 1997, ApJ, 488, L109

- Blaes, O. M. et al. 2001, in the proceedings of "X-ray Emission from Accretion onto Black Holes",  
(<http://www.pha.jhu.edu/groups/astro/workshop2001/papers/blaes.om.ps>)
- Beloborodov, A. M. 1998, MNRAS, 297, 739
- Borozdin, K. et al. 1999, ApJ, 517, 367
- Colbert, E. J. M. and Mushotzky, R. F. 1999, ApJ, 519, 89
- Colbert, E. J. M. and Ptak, A. 2002, ApJS, 143, 25
- Connors, P. A., Piran, T. and Stark, R. F. 1980, ApJ, 235, 224
- Cunningham, C. T. 1975, ApJ, 202, 788
- Dotani, T. et al. 1997, ApJ, 485, L87
- Ebisawa, K., Mitsuda, K. and Hanawa, T. 1991, ApJ, 367, 213
- Ebisawa, K. et al. 1993, ApJ, 403, 683
- Ebisuzaki, T. et al. 2001, ApJ, 562, L19
- Fabbiano, G. 1988, ARA&A, 27, 87
- Foschini, L. et al. 2002, A&A, 392, 817
- Giełiński, M., Maciolek-Niedzwiecki, A. and Ebisawa, K. 2001, MNRAS, 325, 1253
- Grimm, H.-J., Gilfanov, M. and Sunyaev, R. 2003, MNRAS, 339, 793
- Greiner, J., Cuby, J. G. and McCaughrean, M. J. 2001, Nature, 414, 522
- Hanawa, T. 1989, ApJ, 341, 948
- Hubeny, I., Agol, E., Blaes, O. and Krolik, J. H. 2000, ApJ, 533, 710
- Kaaret, P. et al. 2001, MNRAS, 321, L29
- Kato, S., Fukue, J. and Mineshige, S. 1998, "Black-Hole Accretion Disks", Kyoto University Press
- King, A. et al. 2001, ApJ, 552, L109
- Kitamoto, S., Tsunemi, H. and Roussel-Dupre, D. 1992, ApJ, 391, 220

- Körding, E., Falcke, H. and Markoff, S. 2002, A&A, 382, L13
- Kotoku, J. et al. 2000, PASJ, 52, 1081
- Kubota, A. 2001, Doctoral Thesis, University of Tokyo, ISAS Research Note 732.
- Kubota, A. et al. 1998, PASJ, 59, 667
- Kubota, A. et al. 2001, ApJ, 547, L119
- Kubota, A., Makishima, K. and Ebisawa, K. 2001, ApJ, 560, L147
- Krolik, J. H. 1999, "Active Galactic Nuclei", p.151, Princeton University Press
- Laor, A., Netzer, H. and Piran, T. 1990, MNRAS, 242, L560
- Makishima, K. et al. 1986, ApJ, 308, 635
- Makishima K. et al. 2000, ApJ 535, 632
- Matsumoto, H., et al. 2001, ApJ, 547, L25
- Mitsuda, K. et al. 1984, PASJ, 36, 741
- Mizuno, T. et al. 1999, PASJ, 51, 663
- Mizuno, T., Kubota, A. and Makishima, K. 2001, ApJ, 554, 1282
- Okada, K. et al. 1998. PASJ, 50, 25
- Ohsuga, K., Mineshige, S. Mori, M. and Umemura, M. 2002, ApJ, 574, 3150
- Orosz, J. A. and Bailyn, C. D. 1997, ApJ, 477, 876
- Ross, R.R. & Fabian, A. C. 1996, MNRAS, 281, 637
- Ross, R.R. & Fabian, A. C. and Mineshige, S. 1992, MNRAS, 258, 189
- Schwarzschild, M. and Härm R. 1959, ApJ, 129, 637
- Shakura, N. I. and Sunyaev R. A. 1973, A &A, 24, 337
- Shimura, T. and Manmoto, T. 2003, MNRAS, 338, 1013
- Shimura, T. and Takahara, F. 1985, ApJ, 445, 780
- Shrader, C. and Titarchuk, L. 1999, ApJ, 521, L121

- Sobczak, et al. ApJ, 1999, 520, 776
- Strohmayr, T. E. 2001, ApJ, 552, L49
- Sugiho, M. et al. 2001, ApJ, 561, L73
- Sun W. and Malkan, M. A. 1989, ApJ, 346, 68
- Szuskiewicz, E., Malkan, M. A. and Abramowicz, M. A. 1996, 458, 474
- Tanaka, Y. and Lewin, W. H. G. 1995, in “X-ray Binaries”, p. 126, ed. W. H. G. Lewin, J van Paradijs and E. P. J. van den Heuvel, Cambridge Astrophysics Series 26
- Tomsick J. et al. 1999, ApJ, 512, 892
- Wang, D. Q. 2002 MNRAS, 332, 764
- Watarai, K. et al. 2000, PASJ, 52, 133
- Watarai, K., Mizuno, T. and Mineshige, S. 2001, ApJ, 549, L77
- Yamaoka, K. 2001, Doctoral Thesis, University of Tokyo.
- Zhang, S. N., Cui, W. and Chen, W. 1997, ApJ, 482, L155
- Zhang, S. N. et al. 1997, ApJ, 479, 381
- Zhang, S. N. et al. 2000, Science, 287, 1239
- Życki, P. T., Done, C. and Smith, D. A. 2001, MNRAS, 326, 1367

Table 1. GRO J1655-40 fit with Newtonian, Schwarzschild and Kerr disk models<sup>a</sup>

i	Newtonian disk					Schwarzschild disk					Kerr disk ( $\alpha = 0.998$ )						
	$M/M_{\odot}$	$\dot{M}^b$	$\dot{M}/\dot{M}_C^c$	$N_{\text{pow}}^d$	$N_H^e$	$\chi^2/\text{dof}$	$M/M_{\odot}$	$\dot{M}^b$	$\dot{M}/\dot{M}_C^c$	$N_{\text{pow}}^d$	$N_H^e$	$\chi^2/\text{dof}$	$M/M_{\odot}$	$\dot{M}^b$	$\dot{M}/\dot{M}_C^c$	$N_{\text{pow}}^d$	$N_H^e$
0°	1.3	0.49	0.18	7.2	0.97	1.3	0.83	0.37	6.9	0.97	1.35	2.6	0.58	0.48	6.2	0.98	1.40
30°	1.4	0.56	0.19	7.2	0.97	1.3	0.96	0.36	6.0	0.95	1.25	3.0	0.33	0.24	4.0	0.94	1.20
45°	1.6	0.69	0.22	7.2	0.97	1.3	1.2	0.34	5.2	0.93	1.17	5.2	0.36	0.15	3.9	0.94	1.30
70°	2.3	1.42	0.31	7.2	0.97	1.3	1.8	0.40	4.7	0.92	1.08	15.9	0.35	0.048	8.9	0.99	1.45
80°	3.2	2.80	0.43	7.2	0.97	1.3	2.4	0.45	6.3	0.93	1.14	27.0	0.39	0.032	10.4	0.99	1.62

<sup>a</sup>Distance is assumed to be 3.2 kpc, and  $T_{\text{cal}}/T_{\text{eff}}=1.7$ . Slope of the power-law component is fixed to 2.5. One percent systematic error is included for each spectral bin. Degree of freedom (dof) is 156.

<sup>b</sup>Unit is  $10^{18} \text{ g s}^{-1}$ .

<sup>c</sup>The critical mass accretion rate  $\dot{M}_C$  is so defined that  $\dot{M} = \dot{M}_C$  gives the Eddington luminosity. See Appendix A.

<sup>d</sup>Power-law component normalization in photons  $\text{s}^{-1} \text{ cm}^{-2} \text{ keV}^{-1}$  at 1 keV.

<sup>e</sup>In  $10^{22} \text{ cm}^{-2}$ .

Table 2. IC342 Source 1 fit with Newtonian, Schwarzschild and Kerr disk models<sup>a</sup>

<i>i</i>	Newtonian disk					Schwarzschild disk					Kerr disk ( $a = 0.998$ )				
	$M/M_{\odot}$	$\dot{M}^b$	$\dot{M}/\dot{M}_C^c$	$N_H^d$	$\chi^2/\text{dof}$	$M/M_{\odot}$	$\dot{M}^b$	$\dot{M}/\dot{M}_C^c$	$N_H^d$	$\chi^2/\text{dof}$	$M/M_{\odot}$	$\dot{M}^b$	$\dot{M}/\dot{M}_C^c$	$N_H^d$	$\chi^2/\text{dof}$
0°	14.6	170	5.8	0.42	0.91	8.9	304	11.8	0.43	0.90	27.3	195	15.5	0.50	0.91
30°	15.7	197	6.3	0.42	0.91	10.1	335	11.4	0.44	0.90	29.5	106	7.8	0.51	0.90
45°	17.4	241	6.9	0.41	0.91	11.9	387	11.2	0.44	0.90	51.3	113	4.8	0.51	0.90
60°	20.7	341	8.2	0.42	0.91	15.2	502	11.4	0.44	0.89	107	120	2.4	0.46	0.91
80°	35.1	981	14.0	0.42	0.91	25.9	1069	14.2	0.38	0.91	332	153	1.0	0.30	1.00

<sup>a</sup>Distance is assumed to be 4 Mpc, and  $T_{col}/T_{eff}=1.7$ . Degree of freedom (dof) is 52.

<sup>b</sup>Unit is  $10^{18} \text{ g s}^{-1}$ .

<sup>c</sup>The critical mass accretion rate  $\dot{M}_C$  is so defined that  $\dot{M} = \dot{M}_C$  gives the Eddington luminosity. See Appendix A.

<sup>d</sup>In  $10^{22} \text{ cm}^{-2}$ .

Table 3. IC342 Source 1 fit with Slim disk model<sup>a</sup>

$i$	$M/M_{\odot}$	$\dot{M}^b$	$\dot{M}/\dot{M}_C^d$	$L_{disk}/L_{Edd}$	$N_H^d$	$\chi^2/\text{dof}$
$0^\circ$	$19.8 \pm 1.7$	$1000 \pm_{800}^{1300}$	$20 \pm_{16}^{23}$	5.9	$0.90 \pm_{0.06}^{0.08}$	1.40

<sup>a</sup>Distance is assumed to be 4 Mpc, and  $T_{col}/T_{eff}=1.7$ . The viscous parameter  $\alpha = 0.01$ . Degree of freedom (dof) is 52. Errors correspond to 90 % confidence level.

<sup>b</sup>Unit is  $10^{18} \text{ g s}^{-1}$ .

<sup>c</sup>The critical mass accretion rate  $\dot{M}_C$  is so defined that  $\dot{M} = \dot{M}_C$  gives the Eddington luminosity in the case of the standard disk. See Appendix A.

<sup>d</sup>In  $10^{22} \text{ cm}^{-2}$ .

Comparison of Newtonian, Schwarzschild and Kerr disk spectra

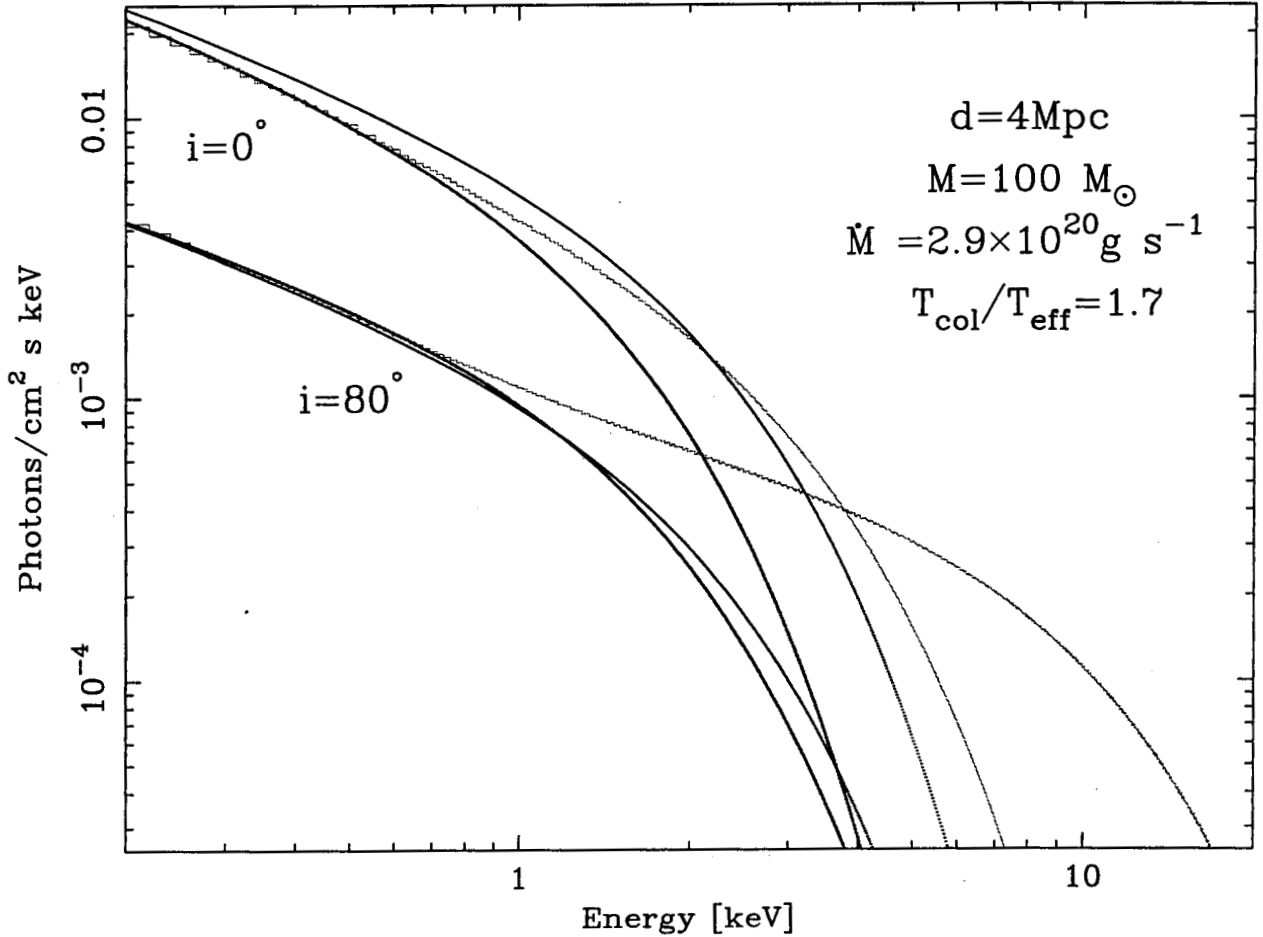


Fig. 1.— Comparison of Newtonian (black), Schwarzschild (red) and extreme Kerr ( $a = 0.998$ ; green) disk spectra for the face-on ( $i = 0^\circ$ ) and a near edge-on disk ( $i = 80^\circ$ ). Inner disk radius is  $6 r_g$  for the Newtonian and Schwarzschild disks, and  $1.24 r_g$  for the Kerr disk. The same mass accretion rate is assumed, which is so chosen to give the Eddington luminosity for the Schwarzschild disk. Other disk parameters are indicated in the figure. Note that the total disk luminosities are different for the three disk models because the energy conversion efficiencies are different (0.083, 0.057 and 0.366 for Newtonian, Schwarzschild and Kerr disks, respectively).

Kerr disk at  $d = 1$  kpc,  $M = 1 M_{\odot}$ , Eddington limit  
 $\mu = 0.9, 0.7, 0.5, 0.3$  and  $0.1$

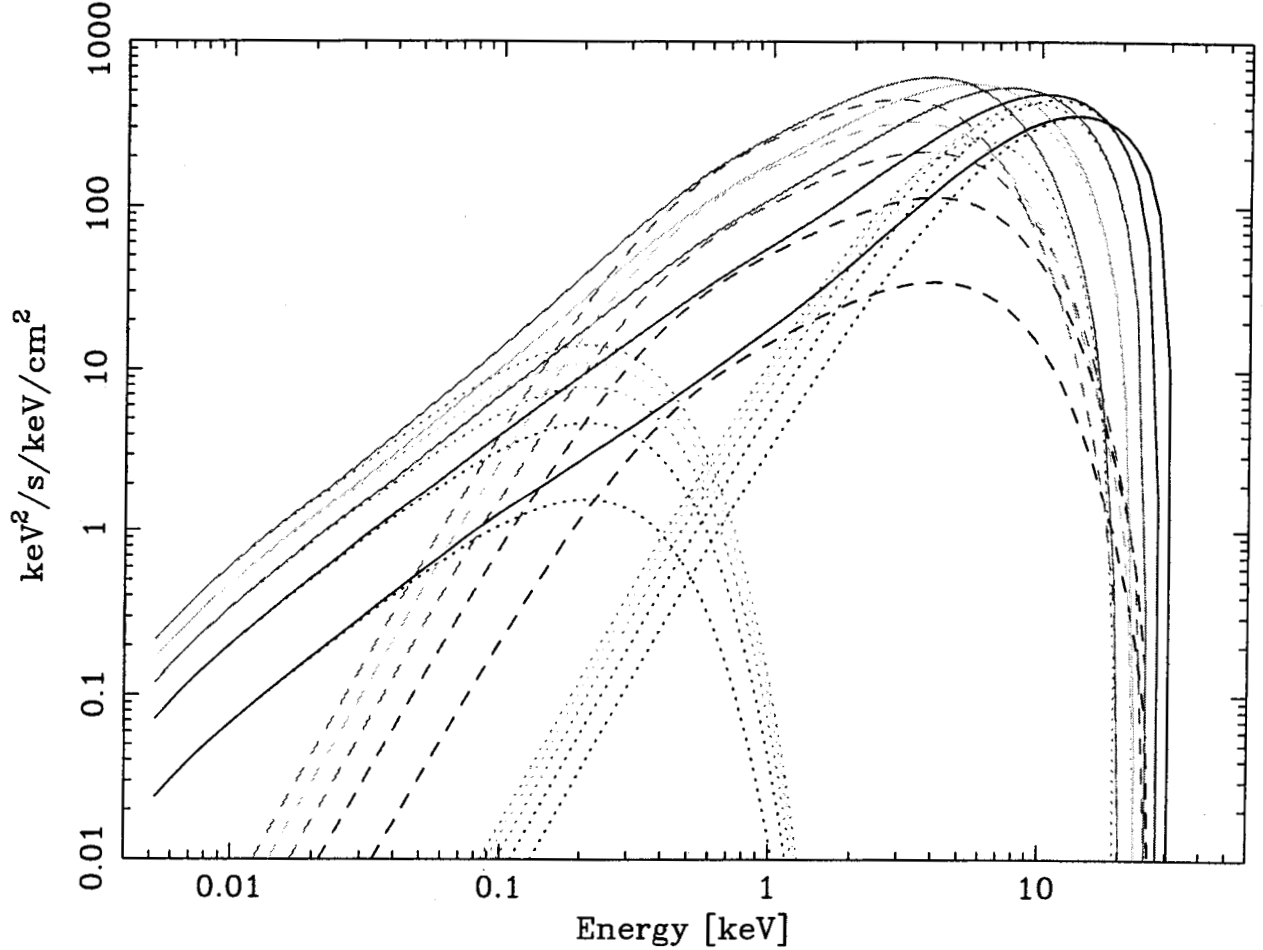


Fig. 2.— The Kerr accretion disk spectra with an extreme angular momentum ( $a = 0.998$ ), observed at the inclination angle  $\mu \equiv \cos i = 0.9$  (green; near face-on),  $0.7$  (yellow),  $0.5$  (cyan),  $0.3$  (red) and  $0.1$  (black; near edge-on). Note the unit of the ordinate ( $\text{keV}^2 \text{ s}^{-1} \text{ keV}^{-1} \text{ cm}^{-2}$ ) which facilitates to see the energy release per logarithmic energy. Solid lines indicate the total disk spectra, and contributions from inner ( $1.26 r_g < r < 7 r_g$ ), middle ( $7 r_g < r < 400 r_g$ ), and outer parts ( $400 r_g < r$ ) are plotted separately either by dotted line or broken line. The distance and mass are assumed to be  $1$  kpc and  $1 M_{\odot}$  respectively. The Eddington luminosity is assumed, and  $T_{col}/T_{eff} = 1$ .

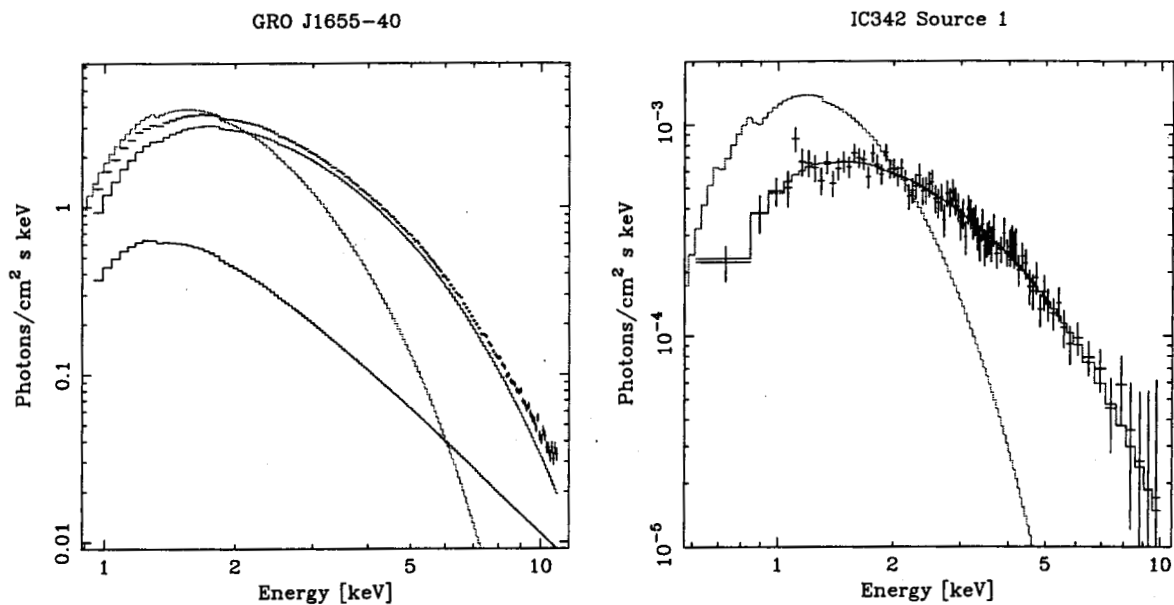
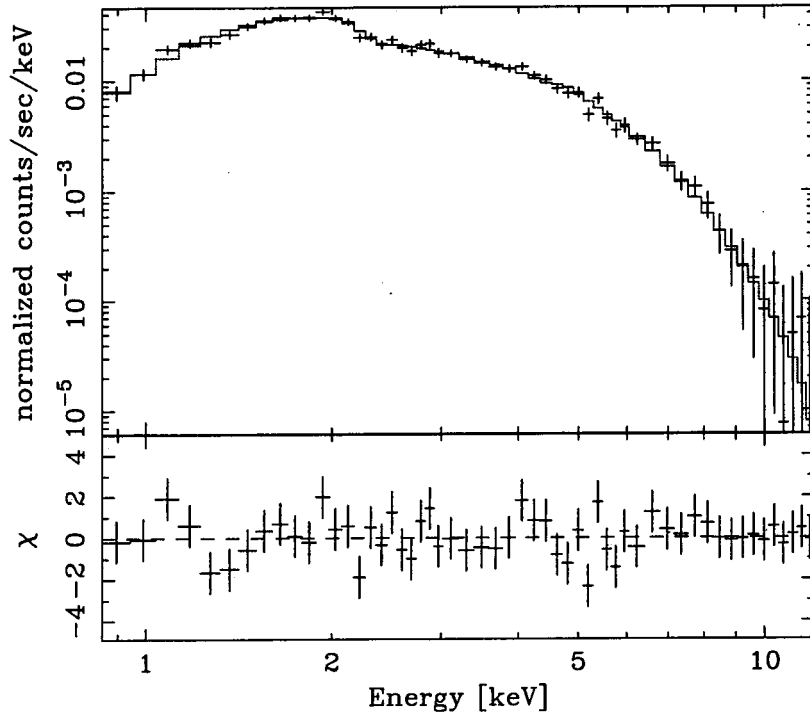


Fig. 3.— ASCA GIS energy spectra of GRO J1655-40 (left panel) and IC342 Source 1 (right). The best-fit Schwarzschild disk models are indicated in red, in which case the best-fit masses are too small ( $1.8 M_{\odot}$  and  $8.9 M_{\odot}$  for GRO J1655-40 and IC342 respectively) compared to the mass determined from optical observations ( $7 M_{\odot}$  for GRO J1655-40), or that expected from the observed luminosity ( $100 M_{\odot}$  for IC342). Schwarzschild disk spectra with the expected masses give too low temperatures to explain the observed accretion disk spectra for both cases (shown in green). Additional power-law component (blue in left panel) is required to fit the GRO J1655-40 spectrum.

IC 342 Source 1; Standard Disk Fit



IC 342 Source 1; Slim Disk Fit

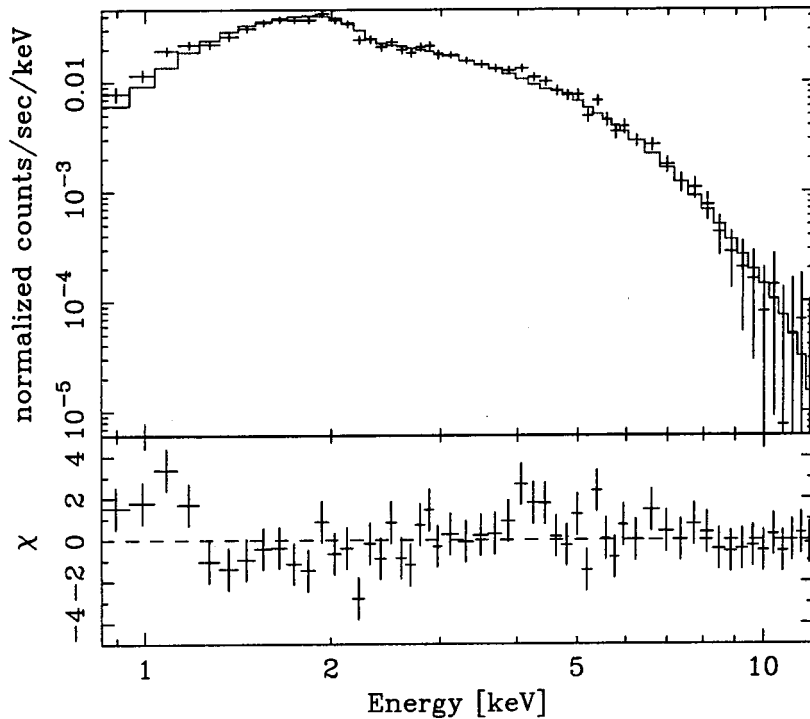


Fig. 4.— IC342 Source 1 ASCA GIS spectrum fitted with the Schwarzschild disk model ( $i = 0^\circ$ ; top) and with the slim disk model (bottom). Residual is more conspicuous in the slim disk model below  $\sim 1.5$  keV.

IC342 Source 1 Best-fit models

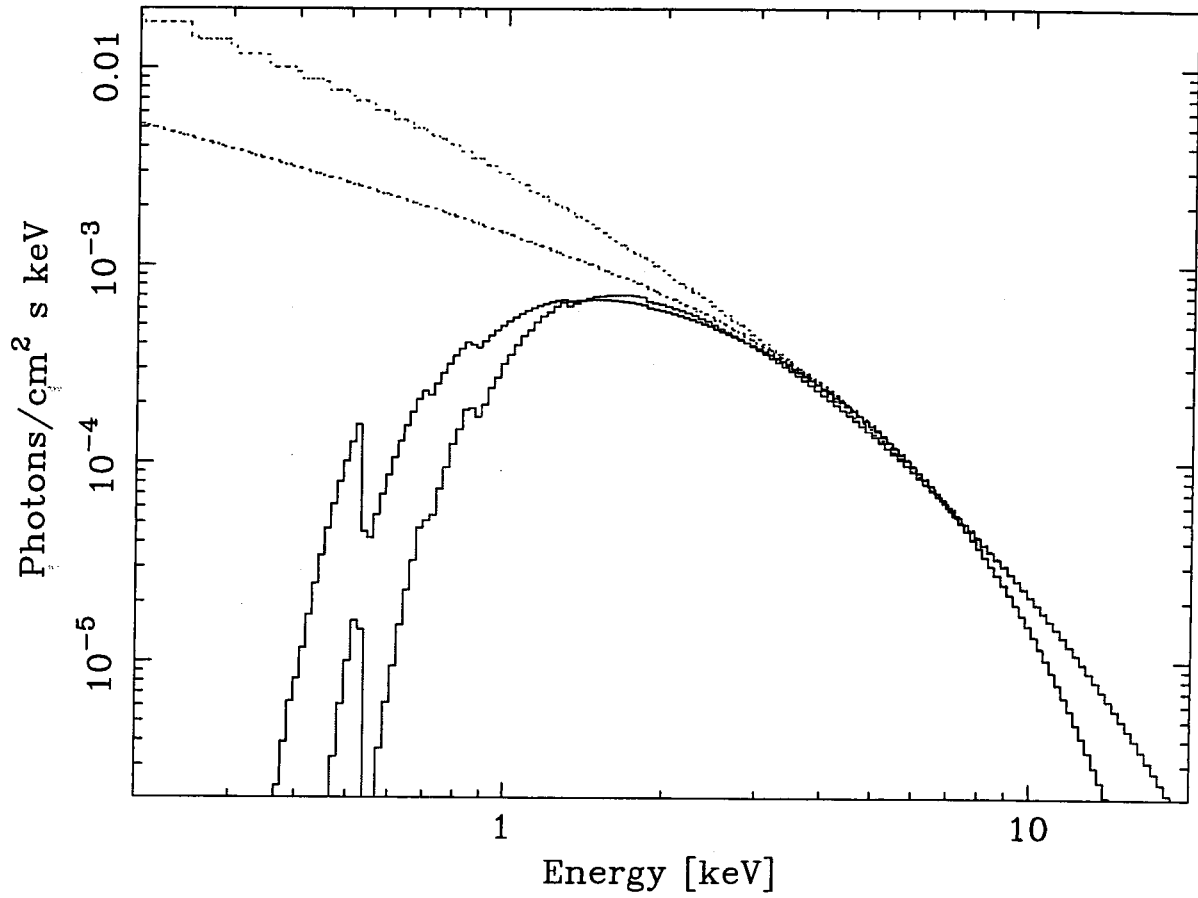


Fig. 5.— IC342 Source 1 best-fit standard accretion disk model (face-on Schwarzschild disk; black) and slim disk model (red). Models removed of interstellar absorption are shown in dotted lines.

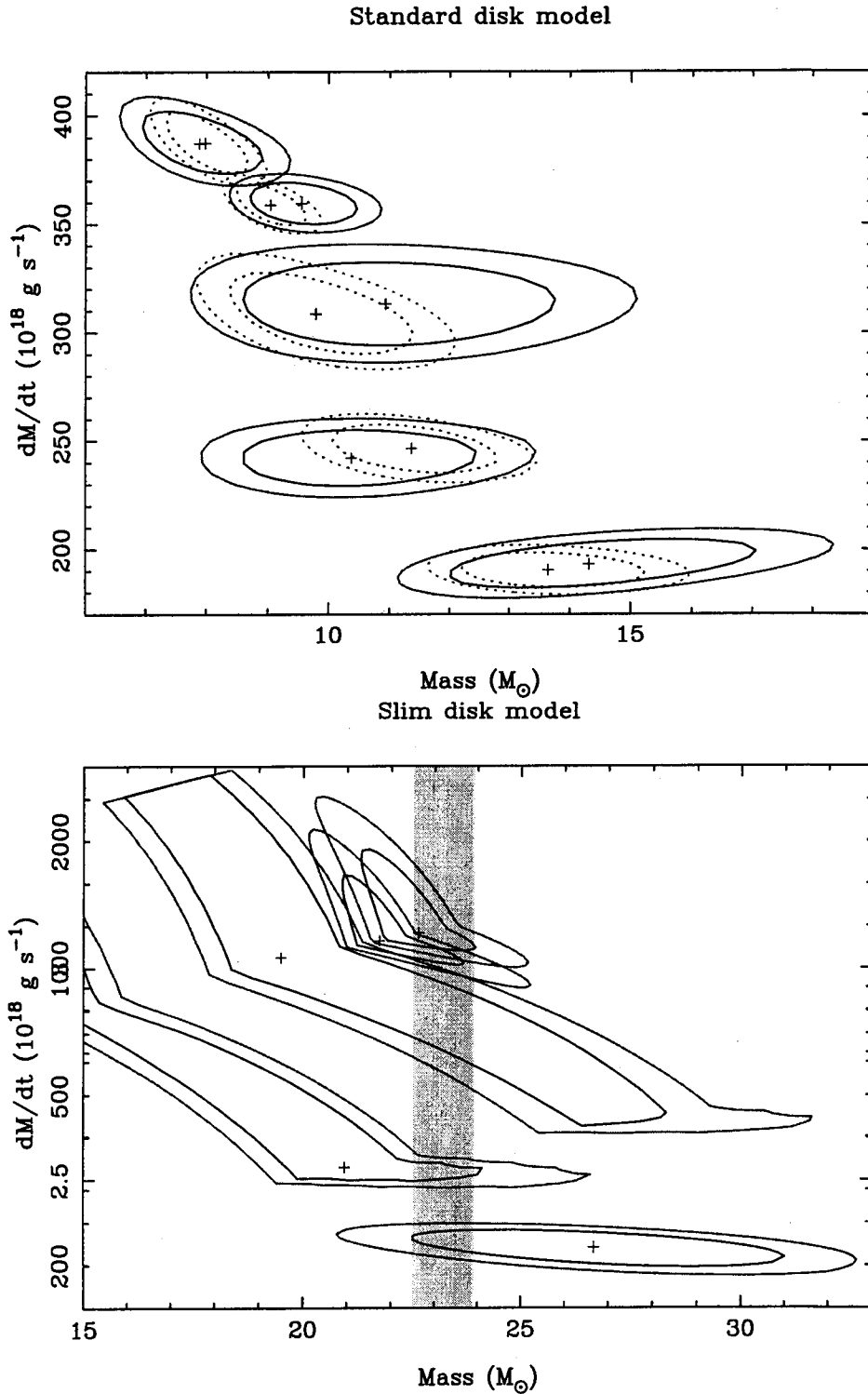


Fig. 6.— Spectral variation of IC342 Source 1 observe in September 1993. The same datasets as in Mizuno, Kubota and Makishima (2001) are used. The upper-panel indicates the variation of mass and mass accretion rates obtained by applying the standard Schwarzschild disk model (GRAD model). Contours with dotted lines are from fitting in 0.5–10 keV, and those with solid lines are from 2–10 keV. The two contour levels indicate 68 % ( $1\sigma$ ) and 90 % error regions for two parameters. The lower panel is obtained through application of the slim disk model in 2 – 10 keV. The region marked with gray indicates that the observed spectral variation is achieved with constant  $M$  and variable mass accretion rates.

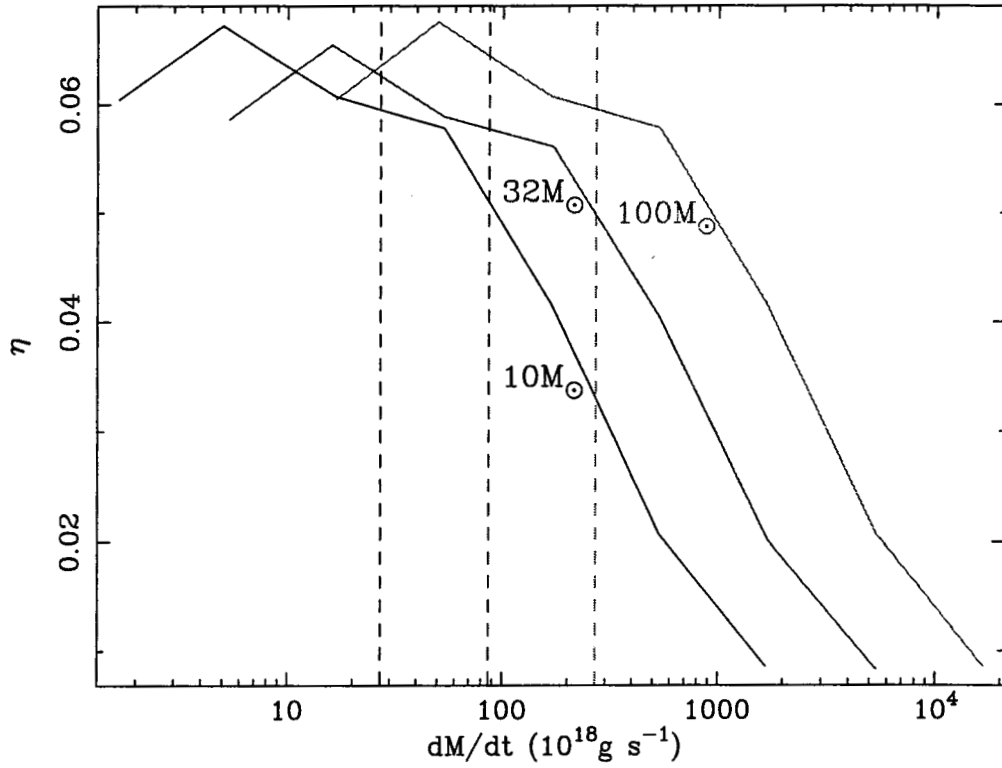


Fig. 7.— Energy conversion efficiency of the slim disk used in the present paper and in Watarai, Mizuno and Mineshige (2001). The vertical broken lines indicate the critical mass accretion rates  $\dot{M}_C$  which gives the Eddington luminosity in the standard disk model (see appendix A).

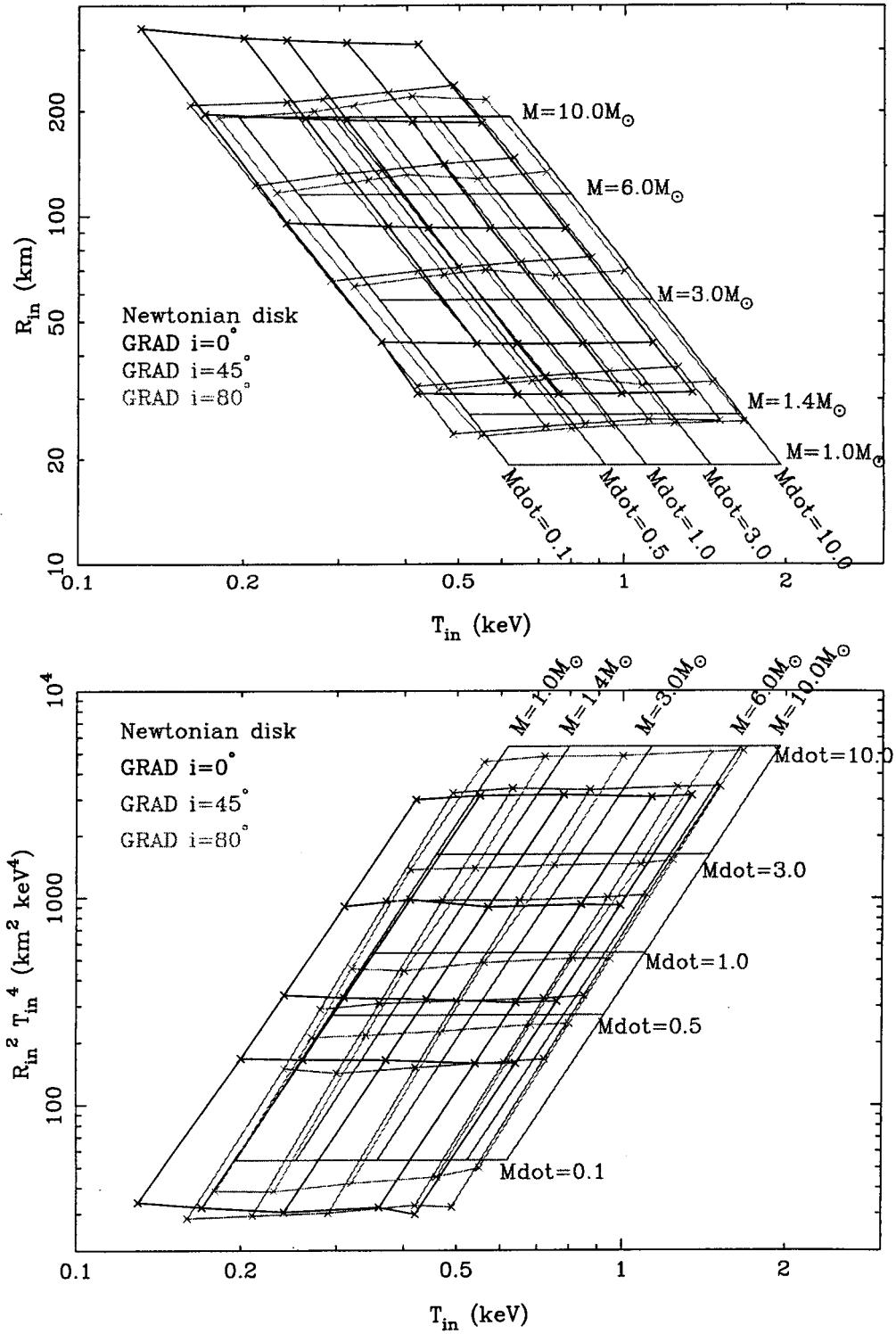


Fig. 8.— Comparison of the Newtonian and Schwarzschild disk spectra through representing these spectra with MCD model parameters. Upper figure shows  $R_{in}$  and  $T_{in}$  values to fit each of the Newtonian or Schwarzschild disk spectra with various mass, mass accretion rate and inclination. Note that  $R_{in}$  is proportional to mass. In the lower figure, ordinate is  $R_{in}^2 T_{in}^4$ , which is proportional to the disk luminosity and mass accretion rate. Unit of the mass accretion rate is  $10^{18} \text{ g s}^{-1}$ . Distance is assumed to be 1 kpc, and  $T_{col}/T_{eff} = 1$ .